

## $g_J$ Factor of the Lowest $^1P_1$ and $^3P_1$ States of Ba; Level-Crossing Determination of $A(^1P_1)/\mu_0 g_J(^1P_1)$ of $\text{Hg}^{199\ddagger}$

MICHAEL W. SWAGEL\*

*Columbia Radiation Laboratory, Columbia University, New York, New York 10025*

AND

ALLEN LURIO

*IBM Watson Laboratory, Columbia University, New York, New York 10025*

(Received 7 December 1967)

The  $g_J(^3P_1)$  and  $g_J(^1P_1)$  factors of the  $(6s6p)$  configuration in barium have been determined in a double-resonance experiment. The ratio  $A(^1P_1)/[\mu_0 g_J(^1P_1)]$  of the  $(6s6p)$  configuration in  $\text{Hg}^{199}$  has been measured in a level-crossing experiment. The results are:  $g_J(^1P_1, \text{Ba}) = 1.0039 \pm 0.0008$ ,  $g_J(^3P_1, \text{Ba}) = 1.4973 \pm 0.0007$ ,  $-\hbar A(^1P_1, \text{Hg}^{199})/[\mu_0 g_J(^1P_1, \text{Hg}^{199})] = 2523.0 \pm 3.0$  G. From the values of  $A(^1P_1, \text{Hg}^{199})$  obtained from optical spectroscopy, a value of  $g_J(^1P_1, \text{Hg})$  is derived:  $g_J(^1P_1, \text{Hg}) = 1.0127 \pm 0.0050$ . We have summarized all lifetime and  $g_J$  values for the first excited  $sp$  configuration of the group-II elements. With these results, a comparison of the three different methods of calculating the intermediate coupling coefficients is presented and all methods are found to be in excellent agreement. Previous level-crossing results for the lifetime and hfs of  $\text{Ba}^{137}$  have been corrected using the presently determined value of  $g_J(^1P_1)$ . These corrected results are in much better agreement with other experiments.

### INTRODUCTION

THE present work is a continuation of our program to investigate the atomic properties of the first excited  $sp$  configuration of the group-II elements. In this paper we describe an experimental determination of the Landé  $g_J$  factor of the  $(6s6p)$   $^1P_1$  and  $^3P_1$  state of barium and the ratio  $A(^1P_1)/g_J(^1P_1)$  for the  $(6s6p)$   $^1P_1$  state of mercury.

From the theory of the  $sp$  configuration<sup>1</sup> it is known that the degree of intermediate coupling of the  $s$  and  $p$  electrons can be determined in three ways, viz.: (1) from the lifetime of the  $^1P_1$  and the  $^3P_1$  states, (2) from the fine structure, and (3) from the  $g_J$  factor of the  $^1P_1$  or the  $^3P_1$  state. It is only in the case of barium and mercury that the  $g_J$  values differ enough from the  $L$ - $S$  coupling values to be useful in estimating the degree of intermediate coupling. The determination of the coupling coefficients from the  $g_J$  values, a comparison with other methods of determining these coefficients, and a test of the  $g$  sum rule, is the object of the present experiment.

The most direct way to obtain the  $g_J$  value is to measure the energy difference between the excited-state Zeeman sublevels of the zero-spin isotopes in an accurately known magnetic field. This we have done by the optical double-resonance technique for the  $^1P_1$  and  $^3P_1$  states of barium. In the case of mercury whose  $^1P_1$  state lifetime is  $1.3 \times 10^{-9}$  sec, the required rf magnetic field necessary to observe double-resonance signals is sufficient to induce a gaseous discharge in the cell. We have therefore resorted to observing the high-field

level-crossing signal in  $\text{Hg}^{199}$ . The magnetic field at which this crossing occurs yields the ratio  $A(^1P_1)/g_J(^1P_1)$ . From recent measurements of  $A(^1P_1)$  by optical spectroscopy<sup>2</sup> and our ratio we can extract  $g_J(^1P_1)$ . Prior to the start of the present work only optical measurements of the  $g_J$  values were available.<sup>3</sup>

### THEORY OF THE EXPERIMENT AND EXPERIMENTAL PROCEDURE

#### A. Barium

The ground state of Ba is  $(6s^2) ^1S_0$  and the first excited configuration is  $(6s6p) ^3P_{2,1,0}$  and  $^1P_1$ . An energy-level diagram of these states is shown in Fig. 1(a). The present double-resonance experiments involve the  $^3P_1$ - $^1S_0$  optical transition at 7911 Å which we shall refer to as the triplet transition, and the  $^1P_1$ - $^1S_0$  optical transition at 5535 Å which we shall refer to as the singlet transition. In the experiments described below, magnetic-dipole transitions are induced between the  $J=1$  state magnetic sublevels of the  $I=0$  isotopes of Ba. The frequency of this transition is  $g_J \mu_0 H / \hbar$ .

A plan of the experimental arrangement is shown in Fig. 2. The light from a hollow cathode lamp was linearly polarized in the horizontal ( $y$ -axis) direction and focused onto a vertical ( $z$ -axis) beam of barium atoms. The barium beam was produced by an oven in a vacuum chamber. The fluorescence was viewed at right angles to both the barium beam and the incident light direction ( $x$  axis) with a photomultiplier. An inter-

<sup>†</sup> This work was supported in part by the Joint Services Electronics Program (U. S. Army, U. S. Navy, and U. S. Air Force) under Contract No. DA-28-043 AMC-00099(E).

\* Present address: Electro-Optical Systems, Inc., 300 North Halstead Avenue, Pasadena, Calif. 91107.

<sup>1</sup> A. Lurio, M. Mandel, and R. Novick, Phys. Rev. **126**, 1758 (1962).

<sup>2</sup> J. Blaise and H. Chantrel, J. Phys. Radium **18**, 193 (1957); T. Duong, S. Gerstenkorn, and P. Luc, in Program and Abstracts of Atomic Spectroscopy Symposium Sponsored by National Bureau of Standards, Washington, D. C., 1967, p. 70 (unpublished).

<sup>3</sup> J. B. Green and R. A. Loring, Phys. Rev. **46**, 888 (1934); T. A. M. Van Kleef and M. Fred, Physica **29**, 389 (1963); C. E. Moore, *Atomic Energy Level Tables*, Natl. Bur. Std. (U.S.), Circ. No. 467 (1949), Vol. III.

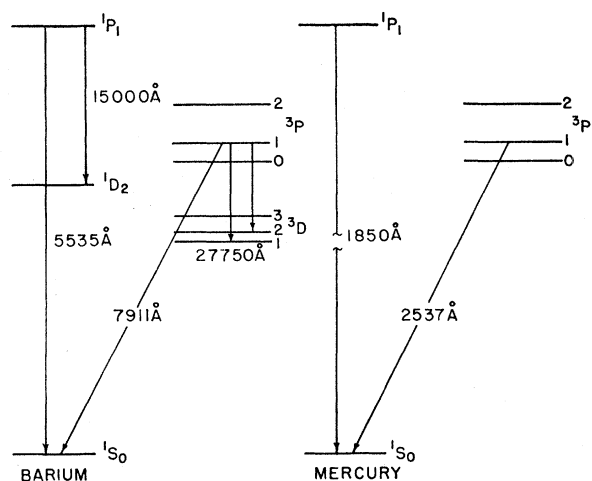


FIG. 1. (a) Ba fine structure; (b) Hg fine structure.

ference filter appropriate to the singlet or triplet transition was located in front of the detector.

A static magnetic field in the  $y$  direction is applied to the atoms in the scattering region by a pair of Helmholtz coils. In the presence of this field only  $\Delta m=0$  transitions are optically excited so that only the  $m=0$  sublevel of the excited  $J=1$  state is populated. The fluorescence produced when the excited atoms in the  $m=0$  state decay has a zero intensity along the  $y$  axis and consequently a minimum of light reaches the detector.

Surrounding the beam in the scattering region is a copper loop which produced an oscillating rf magnetic field in the  $z$  direction. When the static magnetic field is slowly swept through the resonant field condition ( $h\nu_{rf} = g_J\mu_0H$ ), transitions are induced which populate the  $m=\pm 1$  sublevels. The fluorescence produced when these levels decay leads to an increase in the light reaching the detector. This detected resonance signal is used to determine the  $g_J$  value of the excited  $J=1$  states.

In order to enhance the signal-to-noise ratio, a lock-in detection system was used. Resonances were observed both by modulating the static field and by square-wave modulating the amplitude of the rf field. In both cases the frequency of the crystal-controlled oscillator was stable to better than 0.01% and the power stability was better than 1% over the period of a run.

In Fig. 3 we show the atomic-beam chamber for the barium experiment. The source of the beam was a stainless-steel oven heated to  $550^\circ\text{C}$  for the singlet-state measurements and to  $750^\circ\text{C}$  for the triplet-state measurements. The higher beam density for the triplet-state measurements was necessary since the oscillator strength of the  $^1S_0$ - $^3P_1$  transition is 0.0116 while that of the  $^1S_0$ - $^1P_1$  transition is 1.69.

The hollow-cathode lamp, a modification of the Schüller design developed by Bucka,<sup>4</sup> had a barium

<sup>4</sup> H. Schüller, Z. Physik 59, 150 (1930); B. Budick, A. Lurio, and R. Novick, Appl. Opt. 4, 229 (1965).

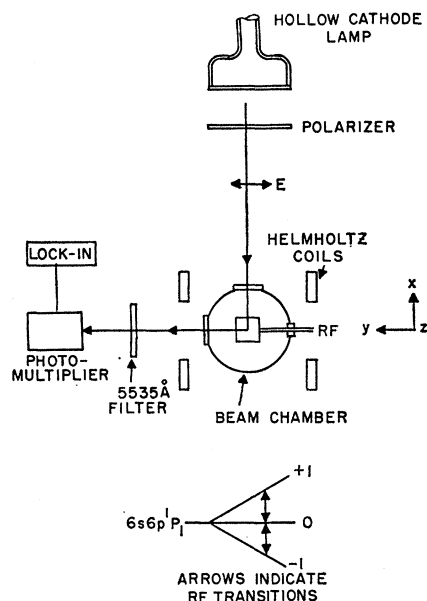


FIG. 2. Schematic plan of apparatus used in barium experiments.

cathode with a  $\frac{3}{8}$ -in.-diam,  $\frac{1}{2}$ -in.-deep hole drilled into it. For optimum signals the dc discharge currents were 170 mA for the singlet line and 350 mA for the triplet line. The argon carrier gas was purified by circulation through a Gehlhoff discharge cell loaded with potassium.

Three sets of mutually orthogonal Helmholtz coils (not shown in Fig. 2) were used to cancel the earth's magnetic field. The applied static field was homogeneous to a part in 30 000 over a 1-in. sphere at the magnet center. It was measured by nuclear magnetic resonance

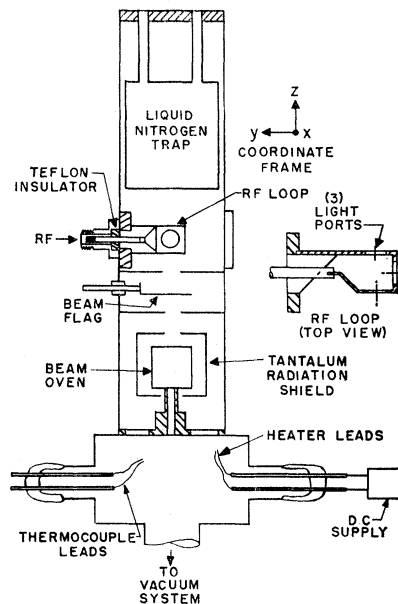


FIG. 3. Details of atomic-beam apparatus used in barium experiment.

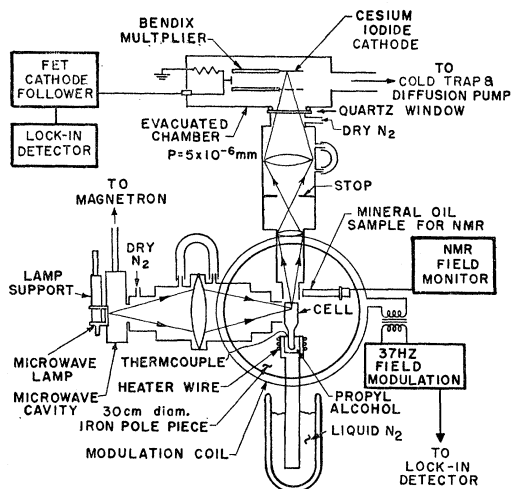


FIG. 4. Details of apparatus used in the level-crossing experiment on the  $^1P_1$  state of mercury. View is in a vertical plane through center of apparatus.

at several field points in order to calibrate a series shunt resistor. In the actual measurements the shunt voltage was used to obtain the magnetic field in the resonance region.

### B. Mercury

The energy-level diagram of Hg is shown in Fig. 1(b). Because the  $^1S_0$ - $^1P_1$  optical transition occurs at 1850 Å, a number of problems peculiar to the far uv region of the spectrum had to be solved. Since 1850 Å radiation is heavily absorbed by oxygen and water vapor, all optical paths had to be flushed continuously with dry nitrogen. We considered a pile-of-quartz-plates polarizer (four plates) but found its transmission loss and poor polarization properties would lead to no significant improvement in the signal-to-noise ratio compared to using unpolarized incident light. The problem of separating the 1850 Å line from the  $^1S_0$ - $^3P_1$  line at 2537 Å was largely overcome by using a cesium iodide photocathode.<sup>5</sup> The quantum efficiency of this cathode is  $8 \times 10^{-5}$  at 2537 Å and  $2 \times 10^{-2}$  at 1850 Å. In addition, the index of refraction of quartz is sufficiently different at these two wavelengths so that selective focusing occurred in our optical system.

In Fig. 4 we show the experimental geometry for the Hg<sup>199</sup> level-crossing experiment. The resonance cell lies between the poles of a 12-in. Varian magnet which was required to attain the 2500-G level-crossing field. The lamp was a reentrant quartz cylinder of 2.5-cm diameter with front and rear faces plane parallel and 2 mm apart having a side arm whose temperature could be controlled. It was excited by being partially inserted into a cylindrical microwave cavity operating at 2.45 GHz.

<sup>5</sup> We are indebted to Dr. H. S. Sommers of the RCA Research Laboratory, Princeton, N. J. for instructing us in the art of preparing these photocathodes.

The quartz resonance cell was filled with a few milligrams of 83% Hg<sup>199</sup>. The optimum level-crossing signal was obtained when the cell side arm was at a temperature of  $-40^\circ\text{C}$  which corresponds to a vapor pressure of about  $1.5 \times 10^{-6}$  Torr. The cell temperature could be held to  $\pm 0.5^\circ\text{C}$  during the period of two field sweeps through the crossing signal. To improve the signal-to-noise ratio the Varian magnet was field modulated by a set of auxiliary coils placed over the poles. The modulation field at 37 Hz was typically operated in the range from 10 to 20 G peak to peak. The magnetic field next to the cell was continuously monitored by proton resonance. Separate measurements indicated that over the region of the cell the field was homogeneous to one part in 4500. No shift was discernable between the field without modulation and the average field with modulation.

The detector was a Bendix electron multiplier with a cesium-iodide-coated cathode. Its output was fed through an FET cathode follower into an EMC<sup>6</sup> lock-in detector and displayed on a recorder.

## OBSERVATIONS AND RESULTS

### A. Barium

Double-resonance signals were recorded at 399.575 and 887.5 MHz for the  $^1P_1$  state and at 399.575 MHz for the  $^3P_1$  state of barium. By applying a small modulation to the static magnetic field and observing the lock-in detector signal, the derivative of a Lorentzian-shaped curve is obtained. By modulating the amplitude of the rf field, a Lorentzian-shaped signal is obtained. The dc magnetic field at the center of these curves would correspond to the resonance field except that the finite integration time used in the lock-in detector introduced a shift in the position of the resonance. If the shift in the field is sufficiently small, quadratic terms in the equation for the shift will be negligible compared to the experimental precision. The linear shift was never larger than 3% of the resonance field and was usually less than 0.5%. In all cases the resonances were averaged by taking both increasing and decreasing field sweeps through the resonance. The observed shift was always in the direction of the field sweep.

Modulation of the dc field produced a background signal which disappeared when the lamp, the beam, or the modulation field was turned off. This signal was probably due to the Zeeman scanning of the atomic absorption across the spectral profile of the lamp. Earlier observations of the dc level of the fluorescence showed a decrease as the magnetic field was increased, indicating that the lamp excitation and cell absorption profiles were, in fact, moving out of coincidence as the

<sup>6</sup> The EMC lock-in detector is manufactured by Electronics Missiles and Communications, 160 East Third Street, Mt. Vernon, N. Y.

TABLE I. Results for barium with varying experimental parameters.

Experimental parameter	$g_J(^1P_1)$	Number of data points	$g_J(^3P_1)$	Number of data points
Field modulation				
399.575 MHz	1.00410±0.00040	5		
887.5 MHz	1.00367±0.00070	7		
Rf amplitude modulation				
399.575 MHz	1.00423±0.00030	4	1.4973±0.0007	9
Rf power 399.575 MHz				
70 W			1.4973±0.0007	1
35 W			1.4973±0.0007	1
25 W			1.4973±0.0007	1
15 W			1.4973±0.0007	1
3 W			1.4972±0.0007	2
Field modulation, 887.5 MHz, at oven temperature				
595°C	1.00369±0.00070	2		
635°C	1.00364±0.00070	2		
Average	1.0039(8)		1.4973(7)	

field was increased. In any event, when the rf field was turned off and the magnetic field was swept over the resonance region, the residual signal was constant over a range of several half-widths at the resonance field, and its effect could be ignored. Also, we found that the results obtained with field and rf amplitude modulation agree to within the stated experimental precision.

Measurements of the  $g_J$  values were made under a variety of experimental conditions in order to disclose any possible systematic errors. In Table I we give the observed  $g_J$  values for different values of radio frequency, rf power, beam oven temperature, and for the two methods of modulation. All of these results overlap within the estimated precision. Variations with rf power and frequency could reveal Bloch-Siegert<sup>7</sup> shifts but this effect was not detected.

Any signal arising from transitions within the odd isotopes of barium should be negligible compared to the signal from the even isotopes. We did not find any indication of these transitions.

Since an rf magnetic field of several gauss is required to produce a detectable double-resonance signal in the  $^1P_1$  state, it was desirable to calibrate roughly the rf field in the loop. The resonance for the triplet state was easily power broadened, and the curve split into two peaks centered about the resonance field. From the static-field difference between the peaks, we obtained an rf field amplitude in the triplet loop of about 1 G when the transmitter rf power was 70 W at 400 MHz. The rf field in the singlet loop at 70 W was about 2 G at 400 MHz.

The Bloch-Siegert shift, which is proportional to the rf power, can be estimated to be

$$\frac{\Delta\nu}{\nu} \approx \frac{H_1^2}{16H_0^2} = \frac{1}{320\,000},$$

where  $\nu = 399.575$  MHz,  $H_0 = 300$  G, and  $H_1 = 2$  G.

<sup>7</sup> F. Bloch and A. Siegert, Phys. Rev. **57**, 522 (1940).

Thus the shift is smaller than the experimental precision, a result which is consistent with the observed independence of the measured  $g_J$  value with rf power variations. The Zeeman interaction of the  $^3P_1$  state with the nearby  $^3P_2$  and  $^3P_0$  fine-structure levels leads to a slight nonlinear magnetic-field dependence of the  $m=0 \rightarrow 1$  and the  $m=0 \rightarrow -1$  transition frequencies. For our experimental conditions these terms contribute only two parts in  $10^5$  of the resonance frequency and in addition shift the two lines by equal and opposite amounts so that the frequency of the line center is independent of these terms. This effect is much smaller in the  $^1P_1$  state.

The greatest possible source of error lies in the determination of the static magnetic field. In deriving an equation relating the shunt voltage to the magnetic field, complete linearity between the field and the shunt voltage was assumed between 100 and 700 G. Although the precision of the field-current data for the  $g_J(^3P_1)$  value is 2.5 parts in 10 000, the precision of the field calibration is estimated to be only five parts in 10 000.

## B. Mercury

Extensive numerical analysis was necessary to determine the ratio  $A(^1P_1)/[\mu_0 g_J(^1P_1)]$  from the level-crossing data. These data consist of seventeen sets of derivative-shaped level-crossing curves; one set of data is defined as the two level-crossing curves produced by sweeping the field through the level-crossing field in first an increasing and then a decreasing direction. The data were taken at cell temperatures ranging from  $-31$  to  $-42^\circ\text{C}$ , corresponding to pressures of  $6 \times 10^{-6}$  and  $1.3 \times 10^{-6}$  Torr, respectively.

In the analysis of the data, it is necessary to determine what point on the curve represents the level-crossing field. The level-crossing signal is superimposed on a fluorescence background that slowly changes as the increasing magnetic field decouples **I** and **J**. As a result

TABLE II. Comparison of present experimental results with previous data.

	$g_J(^1P_1, \text{Ba})$	$g_J(^3P_1, \text{Ba})$	$A(^1P_1, \text{Hg})/$ $g_J(^1P_1, \text{Hg})$ (MHz)
Present work	1.0039(8)	1.4973(7)	3533.2(4.5)
Other results	1.025(8) <sup>a</sup>	1.49651(8) <sup>b</sup>	3532.9(3.3) <sup>c</sup>

<sup>a</sup> H. Bucka and H. J. Schüssler, Ann. Physik 7, 225 (1961).  
<sup>b</sup> J. Ma, J. Mertens, G. Zu Putlitz, and G. Schütte, Z. Physik 208, 266 (1968).  
<sup>c</sup> D. Lecler and J. Margerie, Compt. Rend. Acad. Sci. Paris 265, 123 (1967).

the field where the center of the experimental level-crossing signal occurs does not coincide with the field where the sublevels intersect. In most level-crossing experiments this shift is negligible, but in this experiment the level crossing is so wide that this shift must be considered. We therefore made use of a program developed by Happer<sup>8</sup> which diagonalizes the  $^1P_1$  state hyperfine Zeeman Hamiltonian as a function of magnetic field and with the resulting eigenfunctions calculates the rate  $R$  of fluorescent scattering from the Breit<sup>9</sup> formula and also  $dR/dH$ , the lock-in signal. From plots of  $dR/dH$  in the region of the level-crossing field  $H_c$  and our approximate knowledge of  $A(^1P_1)$  and  $g_J(^1P_1)$  we find  $H_c = H_{\text{midpoint}} + X_1$ , where  $H_{\text{midpoint}}$  is the field halfway between the derivative curve maxima and minima and  $X_1 \approx 0.5$  G.

The absorption of 1850 Å light through the cell was roughly measured and found to vary linearly with field in the region of the level-crossing field. This profile scanning effect will only add a constant term to  $dR/dH$ , the lock-in signal, and so to first order can be ignored. A misalignment in the optical system will produce a shift that could be calculated from the resulting asymmetry in the lock-in detector signal. This effect was examined and found to produce a shift in  $H_c$  of about  $1 \pm 1$  G.

The Zeeman interaction between the  $^1P_1$  state and other nearly fine-structure levels is negligible within our experimental precision. Our final result for the crossing field is  $H_c = 2523.0 \pm 3.0$  G.

TABLE III. Optical spectroscopic measurements of  $A(^1P_1)$  for stable odd isotopes of mercury. Value in parenthesis is inferred; see text.

Author	$A(^1P_1, \text{Hg}^{199})/c$	$A(^1P_1, \text{Hg}^{201})/c$
Blaise and Chantrell <sup>a</sup>	-199.20 mK	43.91 mK
Duong and Gerstenkorn and Luc <sup>a</sup>	(-119.29) mK	44.1 ± 0.2 mK

<sup>a</sup> See Ref. 2.

<sup>8</sup> This program was kindly lent to us by Professor W. Happer of Columbia University.

<sup>9</sup> G. Breit, Rev. Mod. Phys. 5, 91 (1933); P. A. Franken, Phys. Rev. 121, 508 (1961).

## DISCUSSION OF RESULTS

In Table II we compare our experimental results with previous measurements. We have obtained  $A(^1P_1, \text{Hg})/g_J(^1P_1, \text{Hg})$  from our data by making use of the relation

$$H_c = - \frac{hA(^1P_1, \text{Hg})}{\mu_0 g_J(^1P_1, \text{Hg})} \left( 1 + \frac{g_I}{2g_J} \right)^{-1}$$

In this expression  $g_I$  is negative for  $\text{Hg}^{199}$ , and we have taken  $g_J$  to be positive for the electron. It is seen that all the results are in good agreement except for  $g_J(^1P_1, \text{Ba})$  which disagrees with the less precise measurements of Bucha and Schüssler.<sup>10</sup> Their  $g_J$  was obtained from double-resonance experiments at 60 MHz where the rf magnetic field and the line width are comparable to the dc field. It is possible that the Bloch-Siegert effect could explain this discrepancy.

Previous results by Lurio<sup>11</sup> for the lifetime and hfs of the  $^1P_1$  state of  $\text{Ba}^{137}$  which made use of the Bucha and Schüssler  $g_J$  result can now be corrected. The corrected values are  $\tau(^1P_1, \text{Ba}) = 8.37 \pm 0.20 \times 10^{-9}$  sec and  $A(^1P_1, \text{Ba}^{137}) = 110.9 \pm 1.0$  MHz. These new values are in much better agreement with other measurements.

One can obtain  $g_J(^1P_1, \text{Hg})$  from the results in Table II provided  $A(^1P_1, \text{Hg}^{199})$  is known. Two optical spectroscopic experiments have been conducted elsewhere for the determination of  $A(^1P_1, \text{Hg})$  in the odd stable isotopes of mercury. These results are listed in Table III. In order to make use of Gerstenkorn's value of  $A(^1P_1, \text{Hg}^{201})$  we need to calculate from it  $A(^1P_1, \text{Hg}^{199})$ . Although the ratio of the magnetic moments,<sup>12</sup>  $g_I(\text{Hg}^{201})/g_I(\text{Hg}^{199}) = -0.36914$ , is known precisely, we cannot make use of it directly because of the hfs anomaly. However, the principle contribution to all the  $^1P_1$  and  $^3P_1$  hfs comes from the  $s$  electron so we may use the averaged ratio<sup>13</sup>

$$A(^3P_2, \text{Hg}^{201})/A(^3P_2, \text{Hg}^{199}) \cong A(^3P_1, \text{Hg}^{201})/A(^3P_1, \text{Hg}^{199}) \approx -0.3697$$

TABLE IV.  $g_J$  values for mercury and barium and a test of the  $g$  sum rule.

Quantity	Mercury	Barium
$g_J(^1P_1)_{\text{expt}}$	1.0127 ± 0.005	1.0039 ± 0.0008
$g_J(^3P_1)_{\text{expt}}$	1.486107 ± 0.000012	1.4973 ± 0.0007
$[g(^1P_1) + g(^3P_1)]_{\text{expt}}$	2.4988	2.5012
$[g(^1P_1) + g(^3P_1)]_{\text{theor}}$	2.5012	2.5012

<sup>10</sup> H. Bucka and H. J. Schüssler, Ann. Physik 7, 225 (1961).

<sup>11</sup> A. Lurio, Phys. Rev. 136, A376 (1964).

<sup>12</sup> A. Lindgren, in *Perturbed Angular Correlations* (North-Holland Publishing Co., Amsterdam, 1964), Appendix, p. 379; see also V. W. Cohen and G. H. Fuller, in *Nuclear Data Sheets*, compiled by K. Way *et al.* (National Academy of Sciences—National Research Council, Washington, D. C., 1965), Appendix I.

<sup>13</sup> M. N. McDermott and R. Novick, Phys. Rev. 131, 707 (1963); C. Stager, *ibid.* 132, 275 (1963); R. Kohler, *ibid.* 121, 1104 (1961).

TABLE V. Summary of lifetime and Landé  $g_J$  factors for the group-II elements. The listed experimental values are averaged over the best experimental results. The references are to original work or articles which summarize previous work.

Z	Element	$\tau(^1P_1)$ (Sec)	$\tau(^3P_1)$ (Sec)	$g_J(^1P_1)$	$g_J(^3P_1)$
80	Mercury	$1.34(4) \times 10^{-9}$ <sup>a,b</sup>	$1.15(2) \times 10^{-7}$ <sup>b</sup>	1.0127(50) <sup>c,d</sup>	1.486120(27) <sup>e</sup>
56	Barium	$8.37(20) \times 10^{-9}$ <sup>f,g</sup>	$1.21(12) \times 10^{-6}$ <sup>h</sup>	1.0039(8) <sup>c</sup>	1.49651(7) <sup>e,i</sup>
48	Cadmium	$1.66(5) \times 10^{-9}$ <sup>j</sup>	$2.39(4) \times 10^{-6}$ <sup>k</sup>	...	1.499846(13) <sup>l</sup>
38	Strontium	$4.77(20) \times 10^{-9}$ <sup>g,m</sup>	$2.1(3) \times 10^{-6}$ <sup>n</sup>	...	1.50065(4) <sup>i</sup>
30	Zinc	$1.40(4) \times 10^{-9}$ <sup>m</sup>	$2.0(2) \times 10^{-6}$ <sup>m</sup>	...	1.500984(20) <sup>e</sup>
20	Calcium	$4.59(11) \times 10^{-9}$ <sup>g,m,p</sup>	$3.67 \times 10^{-4}$ <sup>q</sup>	...	1.50105(7) <sup>r</sup>
12	Magnesium	$2.01(6) \times 10^{-9}$ <sup>m,p</sup>	$2.1(4) \times 10^{-3}$ <sup>s</sup>	...	...

<sup>a</sup> P. Jean, M. Martin, and D. Lecler, *Compt. Rend. Acad. Sci. Paris* **264**, 1791 (1967).

<sup>b</sup> A. Lurio, *Phys. Rev.* **140**, A1505 (1965).

<sup>c</sup> Present work.

<sup>d</sup> D. Lecler and J. Margerie, *Compt. Rend. Acad. Sci. Paris* **265**, 123 (1967).

<sup>e</sup> W. W. Smith, *Phys. Rev.* **137**, A330 (1965).

<sup>f</sup> A. Lurio, *Phys. Rev.* **136**, A376 (1964).

<sup>g</sup> E. Hulpke, E. Paul, and W. Paul, *Z. Physik* **177**, 257 (1964).

<sup>h</sup> H. Bucka and H. H. Nagel, *Ann. Physik* **8**, 329 (1961).

<sup>i</sup> J. Ma, J. Mertens, G. Zu Putlitz, and G. Schütte, *Z. Physik* **208**, 266 (1968).

<sup>j</sup> A. Lurio and R. Novick, *Phys. Rev.* **134**, A608 (1964).

<sup>k</sup> F. Byron, M. N. McDermott, and R. Novick, *Phys. Rev.* **134**, A615 (1964).

<sup>l</sup> R. Kohler and P. Thaddeus, *Phys. Rev.* **134**, A1204 (1964).

<sup>m</sup> A. Lurio, R. L. DeZafra, and R. Goshen, *Phys. Rev.* **134**, A1198 (1964).

<sup>n</sup> J. Ma, G. Zu Putlitz, and G. Schütte, *Z. Physik* **208**, 276 (1968); F. Ackermann, M. Baumann, and J. Gayler, *Z. Naturforsch.* **21a**, 664 (1966).

<sup>o</sup> A. Landman and R. Novick, *Phys. Rev.* **134**, A56 (1964).

<sup>p</sup> W. W. Smith and A. Gallagher, *Phys. Rev.* **145**, 26 (1966).

<sup>q</sup> V. K. Prokof'ev, *Z. Physik* **50**, 701 (1928); see also footnote m, but note that the lifetime ratio in Table II is inverted.

<sup>r</sup> E. W. Otten, *Z. Physik* **170**, 336 (1962).

<sup>s</sup> G. Boldt, *Z. Physik* **150**, 205 (1958); L. A. Vainshtein and I. A. Polevktov, *Opt. i Spektroskopiya* **12**, 460 (1962) [English transl.: *Opt. Spectry. (USSR)* **12**, 254 (1962)] (this paper quotes a result but gives no reference).

to obtain the number shown in parentheses in Table III. With the averaged value of the two results for  $A(^1P_1, \text{Hg}^{199})$  we find  $g_J(^1P_1, \text{Hg}) = 1.0127 \pm 0.0050$ .

In Table IV we list the  $g_J$  values for the  $^1P_1$  and the  $^3P_1$  states of Hg and Ba and examine how well the  $g_J$

sum rule is satisfied. We see that the  $g$  sum rule is satisfied to within an uncertainty of the size of the neglected relativistic and diamagnetic corrections.

Finally in Table V we list the "best" averaged results for the  $g_J$ 's and lifetimes of the  $^3P_1$  and  $^1P_1$  states of all the group-II elements, and in Table VI we compare results for the different ways of calculating the intermediate coupling coefficients. The different methods of calculating the coefficients are summarized by Lurio, Mandel, and Novick.<sup>1,14</sup> It is seen that the agreement in all cases is very good. In view of this good agreement it should be possible to extract the diamagnetic and relativistic corrections for the  $^3P_1$  and  $^1P_1$  states by correcting the measured  $g_J$  values in these states for the amount of mixing due to intermediate coupling. This assumes, of course, that configuration interaction effects are negligible.

#### ACKNOWLEDGMENT

We would like to thank Professor R. Novick for his advice and encouragement during the course of these experiments.

TABLE VI. Intermediate coupling coefficients calculated by the three different methods given by Lurio *et al.*<sup>a</sup>. The fine-structure intervals were taken from Moore's tables.<sup>b</sup>

Element	Method	$C_1$	$C_2$	$\alpha$	$\beta$
Mercury	Lifetimes	0.4293	0.9031	0.9853	-0.1709
	$g_J(^3P_1)$	0.4272	0.9041	0.9849	-0.1732
	Fine structure	0.4412	0.8974	0.9875	-0.1579
Barium	Lifetimes <sup>c</sup>	0.4938	0.8695	0.9950	-0.0995
	$g_J(^3P_1)$	0.4961	0.8682	0.9954	-0.0962
	Fine structure	0.5000	0.8660	0.9958	-0.0917
Cadmium	Lifetimes	0.5402	0.8415	0.9990	-0.0448
	Fine structure	0.5383	0.8428	0.9989	-0.0471
	Strontium	Lifetimes	0.5546	0.8321	0.9996
Fine structure		0.5519	0.8339	0.9995	-0.0309
Zinc		Lifetimes	0.5655	0.8247	0.9999
	Fine structure	0.5656	0.8247	0.9999	-0.0143
	Calcium	Lifetimes	0.5717	0.8204	0.99997
Fine structure		0.5709	0.8210	0.99997	-0.0079
Magnesium		Lifetimes	0.5757	0.8176	1.0000
	Fine structure	0.5742	0.8187	1.0000	-0.0039

<sup>a</sup> Reference 1.

<sup>b</sup> Reference 3.

<sup>c</sup> In this case we must take account of the branching of the  $P$  states to the lower-lying  $D$  states. See footnote f of Table V and note inversion error in Table III of footnote f.

<sup>14</sup> Hugh C. Wolfe, *Phys. Rev.* **41**, 443 (1932); H. Kopferman, *Nuclear Moments* (Academic Press Inc., New York, 1958), 2nd ed., Sec. 29.